Polym. Bull. (2011) 66:351–362
DOI 10.1007/s00289-010-0335-5

ORIGINAL PAPER

Adhesion force between aramid fibre and aramid fibrid by AFM

Sufeng Zhang · Meiyun Zhang · Kecheng Li

Received: 18 March 2010 / Revised: 17 June 2010 / Accepted: 28 June 2010 /
Published online: 11 July 2010

Abstract Understanding the interactive force and bonding force between aramid fibres and fibrids is important in design wet forming and hot pressing technologies for manufacturing aramid paper sheet and in producing the paper sheets of desirable properties. In this study, the morphology of both aramid fibres and fibrids were observed with SEM and atomic force microscopy (AFM). The adhesion force between aramid fibres and fibrids were measured by AFM with a small piece of fibrid attached to a regular AFM tip. The results show that the adhesion force between aramid fibrid and fibrid is 9.20 ± 0.86 nN and that between fibrid and fibres is 1.71 ± 0.42 nN. This explains the importance of the fibrids in the aramid paper sheet in helping bonding between the aramid fibres and gives the resulting sheet a strong physical structure. The adhesion force measured by AFM was confirmed by a theoretical calculation with the Derjaguin–Müller–Toporov (DMT) theory.

Keywords Aramid fibre · Fibrids · Adhesion force · Atomic force microscopy · Tip modification

S. Zhang (✉) · M. Zhang
Key Laboratory of Auxiliary Chemistry & Technology for Chemical Industry, Ministry of Education, College of Papermaking Engineering, Shaanxi University of Science & Technology, Xi'an, Shaanxi 710021, China
e-mail: zhangsufeng@sust.edu.cn; sufengzhang@126.com

M. Zhang
e-mail: myzhang@sust.edu.cn

S. Zhang · K. Li
Department of Chemical Engineering, University of New Brunswick, Fredericton, NB E3B 6C2, Canada
e-mail: kecheng@unb.ca

Introduction

Poly-*m*-phenylene isophthalamide (PMIA), also referred to as polyamide or aramid, consists of alternating benzene rings and amide groups along the chain axis. The aromatic rings serve as the structural backbone, and the intermolecular hydrogen bonds hold the chains together. The combination of a rigid chemical structure with the strong hydrogen bonds results in high thermal, mechanical and chemical stability. Figure 1a shows the structure of aramid, Fig. 1b is a classical model proposed by Piyarat et al. [1] of the hydrogen bonds of PMIA. Molecular forces, including van der Waals forces and hydrogen bonds, between fibre surfaces are attributed mainly to the condensed state and interfibre binding of the aramid fibres and fibrids when they are made into materials such as aramid sheets.

Meta-aramid sheets, developed in the 1960s, are made entirely of synthetic meta-aramid polymer [2]. The sheet is composed of the two forms of the aramid polymer: floc or fibre, and fibrids. Floc is short fibre cut from long aramid yarn, which is spun from meta-aramid polymer [3]. Aramid fibrid is essentially the same fibre but modified into a form, which is easily dispersible, and appears like pulp. It is filmy pieces or patches. The term fibrid is derived from the morphology of the material, i.e., it is a fibre-film hybrid. Fibrids provide the dielectric strength and act as binder and filler in the aramid for aramid fibres in the aramid sheet structure [4]. The two furnish materials are combined together by using a wet paper-making process including wet forming and then hot pressing at high temperature and under high pressure to form a solid sheet form.

Atomic force microscopy (AFM) is widely used to image material surface topography on a nanometer scale, or investigate the other surface properties such as chemical, adhesion or elastic properties of a material [5–9]. AFM is able to measure forces ranging from weak van der Waals ($<10^{-12}$ N) to strong covalent bonds (10^{-7} N) [6]. When the AFM tips are functionalized with specific material, the specific interactions such as molecular recognition forces involving organic functional groups can be determined, which is referred to as chemical force microscopy (CFM) [7]. In order to tackle specific chemical interactions, regular AFM tips can be modified or functionalized with self-assembled monolayers (SAMs) that are terminated with specific organic functional groups. It can also be modified by attaching a small piece of the material of interest or a nano particle of

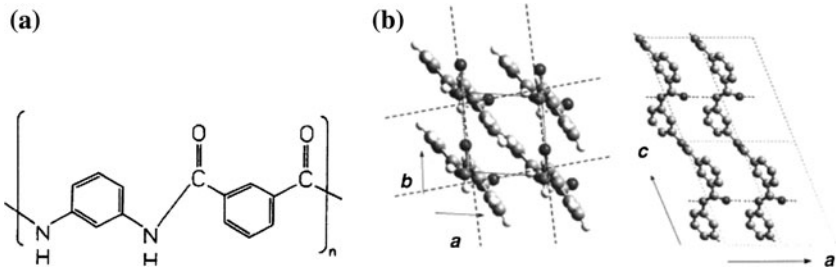

Fig. 1 Chemical structure and hydrogen bonds of aramid in crystal structure of PMIA fibre: **a** chemical structure and **b** hydrogen bonds

the material to the AFM tips [10, 11]. By utilizing chemically functionalized tips, AFM can be used to probe forces between different molecular groups, to measure surface energy on a nanometer scale [12].

Understanding the molecular forces between aramid fibres and aramid fibrids is essential for improving the aramid fibre production process and thus improving the properties of the material. However, very little has been reported in the literature with regard to this. In this study, the interaction forces between aramid fibre and fibrids were measured using AFM. The pull-off adhesion forces (F) between aramid fibres and fibrids were measured by modifying the AFM tip with aramid fibrid film. The work of adhesion (W_A) and surface energy (γ) were calculated from adhesion (pull-off) force (F) by the DMT equation. The results of force measurement were verified by calculating the theoretical force from the experimentally determined contact angle of aramid fibre surface.

Materials and methods

Materials

Aramid fibre and fibrid (PMIA) powders were kindly provided by Anlun Limited Company in China. The average length of the fibres was 6 mm, and the average diameter is about 10 μm. The fibrids were much short, of an average length in one dimension in the range of 0.5–1.8 mm, and a thickness of less than 2 μm. The Canadian Standard Freeness (CSF) of the water suspension was 375 mL.

Scanning electron microscopy (SEM)

The fibre and fibrid surfaces were analyzed using a JEOL JSM-6400 scanning electron microscope in the secondary electrons (SE) mode, with acceleration voltage 10 kV. The spatial resolution was 0.15 μm/pixel. The image size was 1000 × 804 pixels.

AFM

AFM images (512 × 512 pixels) were obtained with an Asylum MFP-3D TS-150 with built-in video microscope, operated in tapping mode in air at room temperature. For AFM imaging, fibres were fixed to a sample holder with double-sided adhesive tape. An Olympus rectangle silicon cantilever with a spring constant 42 N m^{-1} was used. The radius of curvature of the tip was smaller than 10 nm. Images were obtained in height, phase and amplitude modes. Based on the height image, the root mean square (RMS) roughness of the fibrids surface in a scan area of 5 × 5 μm was calculated.

Tip modification

The Veeco NPS tip was modified by directly attaching a small piece of aramid film on it according to [10]. A small amount of epoxy glue (Araldite 10-min

two-component epoxy resin) was carefully spread over the Si_3N_4 pyramidal tip, and aramid films were then glued to the tip. In doing so, a small drop of the mixed resin was spread thinly on one spot of a glass slide with the aid of a plastic ribbon. Aramid fibrid film was placed on another spot of the same slide. The epoxy was spread to form droplets several microns in size. Using the AFM's built-in video system, a small droplet of epoxy resin was applied to the apex of AFM tip. By comparing the size of the epoxy resin droplet on the slide before and after touching with the AFM tip, the amount of resin deposited on the tip was estimated as a few μm^3. After waiting for the epoxy to partially cure ($\sim$5 min at room temperature), the tip was put in contact with aramid film for 1–2 min, and then the tip was disengaged from the slide.

Cantilevers with aramid film attached were placed in an incubator for 24 h at 80 °C to completely cure the epoxy. Each cantilever was then immersed in ultrapure Milli-Q water and ultrasonicated for 10–30 s to eliminate parts that were insufficiently strongly attached.

Measurement of pull-off adhesion forces

Force-distance curves were obtained with the AFM operated in deionized water with pH about 6.50. An NP-S tip (triangular, Si_3N_4 cantilever) with a radius of 20 nm was used in contact mode. The spring constant of the cantilever was 0.58 N m^{-1}. At least 50 force-distance curves were acquired for every tip-sample combination, and any two adjacent measurement points were separated by at least 5 μm on a fibre. For each sample, 5–10 fibres were investigated. The set point, or zero-deflection position in the non-touching regime, was set as the zero-voltage position for all force curves, and the maximum force on the sample surface was kept constant by a trigger mode in the operating system.

Results and discussion

Surface morphology of aramid fibres and fibrids by SEM and AFM

The surface characteristics and properties of aramid fibre and fibrids depend on the manufacturing methods and conditions. The SEM image of the fibres shown in Fig. 2 demonstrates the linear morphology of the fibres, with discontinuous pleats that are fairly uniformly distributed and run parallel to the fibre axis direction.

Better resolution of surface pleat features was obtained by using tapping mode AFM (Fig. 3a). The pleat on the surface of the fibre can be exactly quantified with the height profile image (Fig. 3b). The heights of the pleats are about 80 nm; the RMS roughness is 44.78 nm.

Figure 4 shows the morphology of fibrids in aqueous dispersion by light microscopy, and the morphology in the dry state by SEM. The fibrids are extremely supple in liquid suspension, which permits physical entwining during wet forming in the sheet-making process. A fibrid can be visualized as a soft handkerchief that is about a few hundred microns or less in both length and width dimension (Fig. 4a).

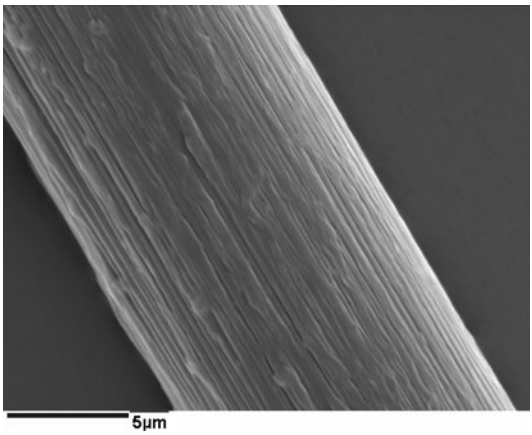

Fig. 2 SEM images of aramid fibre surface

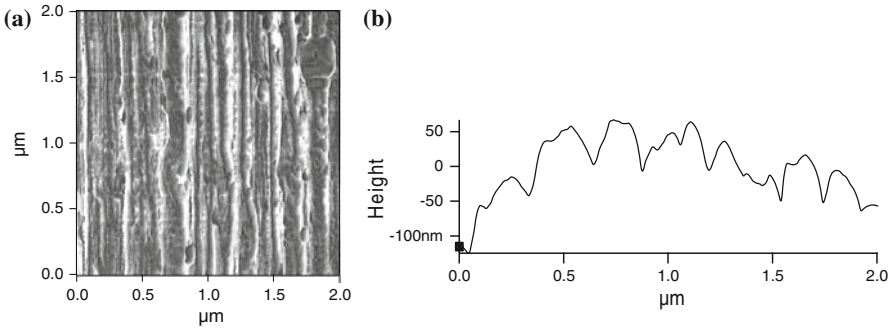

Fig. 3 AFM images of aramid fibre: **a** phase image; **b** height profile obtained from height image (RMS 44.78 nm)

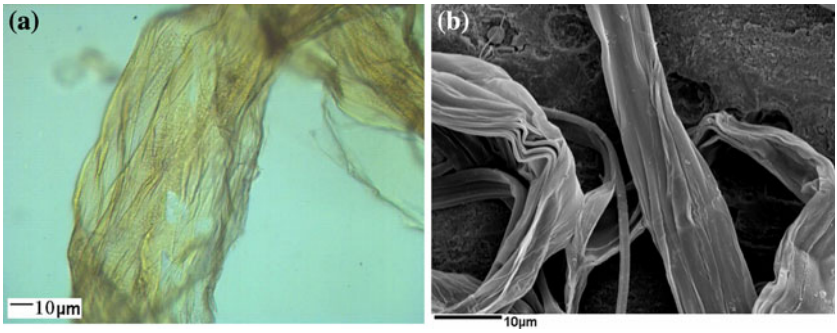

Fig. 4 Morphology of fibrids: **a** a light microscopic image in aqueous suspension; **b** an SEM image in dry state

As opposed to fibres, fibrids are non-rigid filmy, ribbon-like particles with irregular shape. Fibrids have fibrillated-like regions which are more flexible and has less crystallinity. Fibrids have an average size in the range of 0.2–1.0 mm in either one

dimension and a thickness typically of less than 1 μm. The ratio of length or width to the thickness of the fibrids is also very large, ranging from 1000 to 3000. The morphology of fibrids gives them an extremely high specific surface area (up to 300 m^2 g^{-1}) [13], which is beneficial for forming more uniform sheet structure and hence, better sheet physical and thermal properties.

Force measurement on aramid fibres

Tip characterization and calibration

It is important to confirm that a fibrid film is coated on the tip. In doing so, first we observed the coated tip and the original one with SEM. As shown in Fig. 5a, the uncoated original AFM tip is clean with a tip radius approximately 20 nm, and the coated tip had surface covered with the film of fibrids (Fig. 5b). We then compared the adhesion force between the modified tips and the aramid fibre surface and between the original uncoated tips and the same aramid fibre surface using a cantilever of a spring constant of 0.58 N m^{-1}. Each force was an average of about 50 replicate measurements over 1 μm^2 area and the operation was at ambient conditions (relative humidity 54.2%, room temperature 21.2 °C). To obtain absolute adhesion force values, first, the cantilever spring constant has to be calibrated. In addition, the operating such as set point, trigger point and integral gain, have to be optimized and kept constant for the measurements. The smaller the deflection set point, the smaller the deflections of AFM tip. In this experiment the initial deflection set point was set to 1.0 V, integral gain to 10, and trigger point to 0.5 V. The key parameters for force curve measurement, Z-voltage should be slightly in the blue region at about 70 V. The deflection may change to a nonzero value. The results of adhesion force measurements are shown in Fig. 6. The presence of aramid film was inferred from the distinct difference in force values of the coated and uncoated tips. The average adhesion force between the original tips and fibre in air was 13.69 nN, and that between the coated tip and same fibre was 56.28 nN. It is apparent that it is the coated layer, which results in the substantial difference.

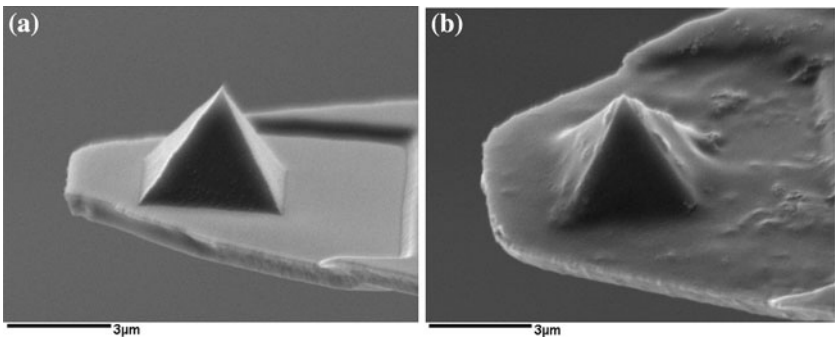

Fig. 5 SEM images of original tip and coated tip: **a** original NPS tip; **b** coated tip

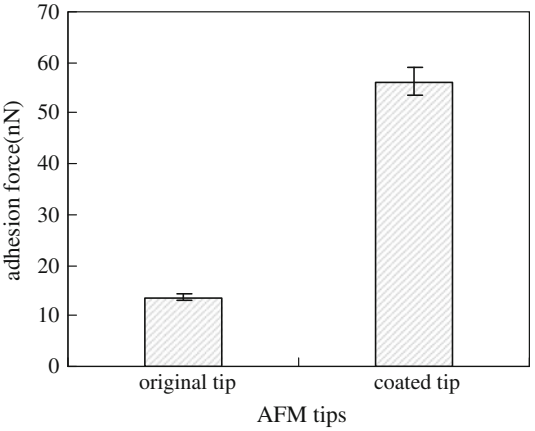

Fig. 6 Adhesion forces between AFM tips and fibres in air

Adhesion force measurement of fibres and fibrids

Under ambient conditions, the interaction forces between the tip and sample is affected not only by the morphology of the sample surface but also by the presence of water between the tip and the sample surface. The water meniscus force arises from capillary condensation and adsorption of thin water films around the contact sites between tip and sample surface [14]. The formation of a meniscus by capillary condensation leads to an attractive force between tip and sample. The total adhesion force F_{adh} measured on the AFM tip is the sum of the capillary force and the interaction forces.

For a sphere tip in contact with a flat surface at high humidity, the capillary force F_{cap} is dependent on humidity and is approximated by the following equation [15]:

$$F_{cap} \approx 4\pi R\gamma \cos\theta \quad (1)$$

where R is the tip radius, γ the surface tension of water (72.6 mJ m^{-2}) and θ the contact angle of water on the sample surface. For $\theta = 63.04°$ (fibre) and 65.28° (fibrid) [16], and $R = 20$ nm, the capillary force F_{cap} is calculated to be 8.27 and 7.63 nN, for the two surfaces, respectively.

In order to avoid the meniscus force between tip and sample due to adsorbed water force measurement were performed in distilled water at pH 6.50. The adhesion forces between aramid fibres and fibrids, and between fibrids and fibrids were measured with an aramid fibrid-coated tip to determine how fibre and fibrids morphology and surface chemistry affect the adhesion force. Adhesion was determined from force of interaction between the functionalized tip and the sample via force-distance curves according to [17]. About 100 force-distance curves were acquired for the lower and higher position on the surface of every sample fibre and fibrids, and both the distribution of adhesion force values measured and the mean adhesion force value were obtained as shown in Fig. 7.

Figure 8 shows typical AFM approach in broken line and retraction in solid line force-distance curves of obtained the fibrid-coated tip on the aramid fibre and the fibrids. The two curves are quite different. When the tip approached the aramid fibre

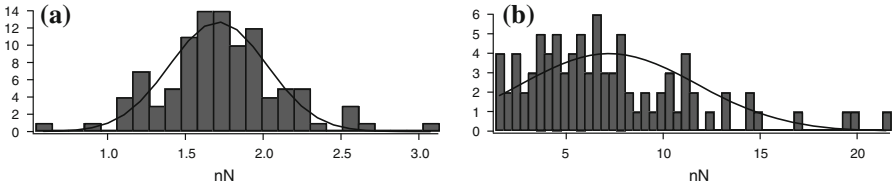

Fig. 7 Distribution of adhesion force values and mean forces: **a** fibrid–fibre; **b** fibrid–fibrid

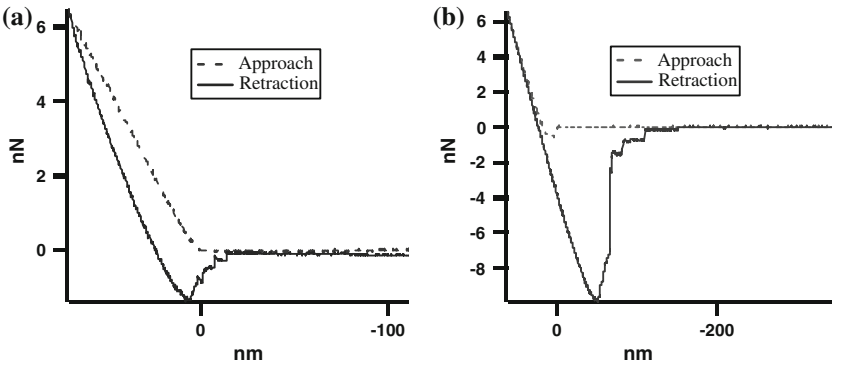

Fig. 8 Typical force-distance curves: **a** fibrid–fibre; **b** fibrid–fibrid

surface, there was no definite "jump on" contact point (Fig. 8a). The profile indicates weak van der Waals and other attractive forces between the modified tip and aramid fibre. This can presumably be explained by the chemical inertness of the fibre due to mainly of high crystallinity of aramid fibres [18, 19]. In comparison, there is a "jump on" force for the modified tip and fibrid surface (Fig. 8b) suggesting a strong attractive force when tip approaches the sample surface. In addition, there is a much larger adhesion peak on the retraction curve, followed by some other small peaks before completely pulled off. The small peaks at the end may be due to the unbinding of the residue weak binding at different layers or distance of the fibrillated parts of the fibrid surface. This is expected because the fibrid surface is very rough and appears hairy on the surface.

The adhesion forces between the aramid fibrid tip and fibre, and that between the tip and fibrid, measured were 1.71 and 9.20 nN nm^{-1}, respectively with a standard deviation of 0.42 and 0.86 nN, respectively. The adhesion force between fibrids and fibrids is more than five times of that between fibrids and fibres. One apparent reason is that the surface of the fibrids is softer and much more compliant than that of the fibres, which will results larger bonded area between the two surfaces, and thus larger absolute adhesion forces. On the other hand, the adhesive force is mainly due to hydrogen bonds between the molecular chains of aramid fibres and fibrids [20]. The microfibrils in fibrids has larger portion of amorphous structure and which has more polar groups on the external surface than the crystal structure on the surface of fibres.

pH-dependence of adhesion force

Amino acids have both acid and base properties, which are responsible for the hydrolysis of aramid fibre in acid or base solution. To support this interpretation, we did some preliminary investigation of the electrostatic interactions between charged surfaces. Knowledge of these Coulombic interactions and the acid–base properties of surfaces are important for understanding phenomena such as interface stability and surface activity. The ionizable functional groups (NH) in the chemical structure of aromatic polyamide allow direct evaluation of charge–charge interactions and determination of the acid–base behaviour of surface acid and base groups [21]. The ionization behaviour of surface-bound amine groups was directly measured by performing pH-dependent adhesion force measurements of the aramid fibrid tip-substrate combination, while maintaining constant ionic strength.

Aqueous electrolyte solutions (1 mM NaCl) with pH ranging from 3.80 to 10.58 were used. After changing pH, equilibrium with the new environment was reached within several minutes. The forces measurement started from neutral pH, then moved to higher pH progressively up to pH 10.58. Then the pH was adjusted to neutral pH and continued progressively to lower pH and down to pH 3.8. The pH was again adjusted back to neutral pH from the lower pH's to check any possible deterioration of the tip, or change of tip geometry, which may cause changes in measured adhesion force.

The measured adhesion forces as a function of the pH of the medium is presented in Fig. 9. It can be seen that at low pH's both tip and substrate have positively charged (NH^+) groups, and hence the measured adhesion forces are very low. At higher pH's the NH groups are recovered, changing the tip-substrate interaction to an attractive hydrogen bonding interaction [22]. As the pH of the medium increases, the NH^+ groups gradually become deprotonated and uncharged or even negatively charged. Because tip and sample bear the same NH functionality, both tip and sample become negatively charged, which results in a repulsive force between the two surfaces. The greater the extent to which the NH^+ groups are deprotonated with increasing pH, the larger this repulsive contribution will be, resulting in a decreasing adhesive force.

Verifying adhesion force by surface energy of the aramid fibre

AFM can provide critical information about surface energy of solids based on adhesion force measurements. For the modified or original tip, the inter-surface free energy γ, or work of adhesion W_A can be calculated, and the relationship between force and γ can be inferred. The present results of force measurement were verified by calculating the theoretical force from the experimentally determined contact angle of the aramid fibre surface.

The adhesion (pull-off) force (F_{adh}) can be described by the Derjaguin approximation

$$F_{adh} = c\pi R W_A \tag{2}$$

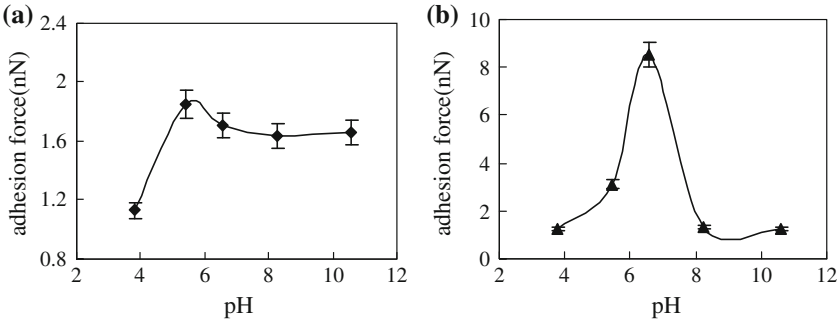

Fig. 9 Adhesion forces between **a** fibrid-coated tips and fibres and **b** fibrid coated tips and fibrids at various pHs

where W_A is the equilibrium work of adhesion to pull the tip off the sample, defined by the negative of the Gibbs free energy change per unit area (ΔG) of the interacting interfaces. R is the radius of the probing tip, and c is a constant, being 2 in the DMT model and 1.5 in the Johnson–Kendall–Roberts (JKR) model. W_A is expressed by the Dupré equation [23]

$$W_A = -\Delta G = \gamma_{tip} + \gamma_{sample} - \gamma_{tip/sample} \tag{3}$$

where γ is the free energy of tip surface or sample surface, or the interfacial free energy of the tip–sample interface. If the tip and the surface are chemically identical, the work of adhesion is $W_A = 2\gamma$, where $\gamma = \gamma_{tip} = \gamma_{sample}$ is the surface free energy of the particular surface in the medium. The interfacial free energy $\gamma_{tip/sample}$ is zero, so

$$F_{adh} = c\pi R \cdot 2\gamma \tag{4}$$

When the surface forces are short range by comparison with the elastic deformations they cause (i.e., compliant materials, strong adhesion forces, large tip radii), the contact area is described by model of the JKR [24]. The other situation (stiff materials, weak adhesion forces, small tip radii) is referred to as the DMT regime [25] and the form of the contact area is presented in the work of Maugis [26]. The DMT theory was used in the present case to calculate the surface free energies from the measured data.

Using Eq. 4, the adhesion force calculated is 9.50 nN for the aromatic polyamide NH–NH tip-sample pair. We used the measured tip radius (20 nm) and the experimental value of γ (40.3 mJ m^{-2}) from contact angle measurements with water on aramid fibrid film surfaces [16]. In comparison with the calculated adhesion force, the measured adhesion force of 9.20 $\pm$ 0.86 nN is in good agreement with the calculated one.

Conclusions

The morphology of both aramid fibres and fibrids were observed with SEM and AFM. It was found that the aramid fibres are rigid, longitudinal and tube-shaped of

about 6 mm in length and 10 μm in diameter, and the aramid fibrid are non-rigid, ribbon-like patches of about 0.2–1.0 mm in one dimension and less than 1 μm in thickness.

The adhesion force between aramid fibres and fibrids were measured by AFM with a small piece of fibrid attached to a regular AFM tip. The results show that the adhesion force between aramid fibrid and fibrid is 9.20 ± 0.86 nN and that between fibrid and fibres is 1.71 ± 0.42 nN. This is probably due to the larger contact area between the fibrids and fibrids than that between fibres and fibres. In addition, the amorphous structure of the fibrids may offer more polarized groups for bonding between the two aramid molecular chains. This explains the importance of the fibrids in the aramid paper sheet in helping bonding between the aramid fibres and gives the resulting sheet a strong physical structure.

The adhesion force measured by AFM was confirmed by a theoretical calculation with the DMT theory.

Acknowledgements Financial support to this research of the National Natural Science Foundation of China (Project NSFC: 50873057), Natural Sciences and Engineering Research Council of Canada (NSERC) and Tianjin Key Laboratory of Pulp & Paper in China (Project 200918) are acknowledged.

References

1. Piyarat N, Kohji T, Yasuhiko M, Orapin R (2002) Factors governing the three-dimensional hydrogen bond network structure of poly(m-phenylene isophthalamide) and a series of its model compounds (I). J Phys Chem 106:6842–6848
2. Bhatia A (1995) Electrical electronics insulation conference, and electrical manufacturing & coil winding conference. Proceedings: 409–410
3. George CG, Waynesboro V (1973) Synthetic paper structures of aromatic polyamides. US Patent 3,756,908
4. Nachinkin OI, D'yakonova ÉB (1971) Fibrous polymeric adhesives from polyvinyl alcohol. Fibre Chem 2(4):410
5. Binnig G, Quate CF, Gerber C (1986) Atomic force microscopy. Phys Rev Lett 56:930–933
6. Israelachvili J (1992) Intermolecular and surface forces. Academic, New York
7. Frisbie CD, Rozsnyai LF, Noy A, Wrighton MS, Lieber (1994) Functional group imaging by chemical force microscopy. Science 265:2071–2074
8. Huang F, Li KC, Kulachinco A (2009) Measurement of interfiber friction force for pulp fibers by atomic force microscopy. J Mater Sci 44:3770–3776
9. Stiernstedt J, Nordgren N, Wågberg L, Brumer H, Gray DG, Rutland MW (2006) Friction and forces between cellulose model surfaces: a comparison. J Colloid Interface Sci 303:117–123
10. Ong OK, Igor S (2007) Attachment of nanoparticles to the AFM tips for direct measurements of interaction between a single nanoparticle and surfaces. J Colloid Interface Sci 310:385–390
11. Noy A, Vezenov DV, Lieber CM (1997) Chemical force microscopy. Annu Rev Mater Sci 27:381–421
12. Jaroslaw D, Garth WT, Elvin RB (2004) Determination of solid surface tension from particle–substrate pull-off forces measured with the atomic force microscope. J Colloid Interface Sci 280:484–497
13. Long H (2001) Study of the rheological properties of Nomex fibrids. Master thesis of the College of Engineering and Mineral Resources at West Virginia University
14. Binggeli M, Mate CM (1994) Influence of capillary condensation of water on nanotribology studied by force microscopy. Appl Phys Lett 65(4):415–417
15. Hans-Jürgen B, Brunero C, Michael K (2005) Force measurements with the atomic force microscope: technique, interpretation and applications. Surf Sci Rep 59:1–152

16. He F, Zhang MY, Zhang SF (2008) Surface energy of aramid fiber/pulp and their sheets property. Acta Materiae Compositae Sinica 25:62–67
17. Weisenhorn AL, Maiveld P, Butt HJ, Hansma PK (1992) Measuring adhesion, attraction, and repulsion between surfaces in liquids with an atomic-force microscope. Phys Rev B 45:11226–11232
18. Yamaguchi T, Kumada H (2006) Method for producing aramid laminate. U.S. Patent 20060127687
19. Allen KW (1987) A review of contemporary views of theories of adhesion. J Adhes 21(3–4):261
20. Zhang SF, Zhang MY, Li KC (2009) Adhesion characteristics of aramid fibre-fibrids in a sheet hot calendering process. Appita J 63(1):58–64
21. Van der Vegte EW, Hadziioannou G (1997) Acid-base properties and the chemical imaging of surface-bound functional groups studied with scanning force microscopy. J Phys Chem B 101: 9563–9569
22. Sprik M, Delamarche E, Michel B, Röthlisberger H, Klein ML (1994) Structure of hydrophilic self-assembled monolayers: a combined scanning tunneling microscopy and computer simulation study. Langmuir 10:4116–4130
23. Houssein A, Gilles C, Maurice B (2005) Quantitative determination of surface energy using atomic force microscopy: the case of hydrophobic/hydrophobic contact and hydrophilic/hydrophilic contact. Surf Interface Anal 37:755–764
24. Johnson KL, Kendall K, Roberts AD (1971) Surface energy and the contact of elastic solids. Proc R Soc London A 324:301–313
25. Derjaguin BV, Muller VM, Toporov YP (1975) Effect of contact deformations on the adhesion of particles. J Colloid Interface Sci 53:314–326
26. Maugis D (1992) Adhesion of spheres: the JKR–DMT transition using a Dugdale model. J Colloid Interface Sci 150:243–269